**Li5(BH4)3NH: Lithium-Rich Mixed Anion Complex Hydride**

# Li5(BH4)3NH, Lithium Rich Mixed Anion Complex Hydride

| | |
|---|---|
| Journal: | *The Journal of Physical Chemistry* |
| Manuscript ID | Draft |
| Manuscript Type: | Article |
| Date Submitted by the Author: | n/a |
| Complete List of Authors: | Wolczyk, Anna ; Universita di Torino, Department of Chemistry<br>Paik, Biswajit; Tohoku Daigaku, IMR<br>Sato, Toyoto; Tohoku University, Institute for Materials Research<br>Nervi, Carlo; University of Torino, Department of Chemistry<br>Brighi, Matteo; Quai Ernest-Ansermet 24, University of Geneva<br>GharibDoust, SeyedHosein; University of Aarhus, Interdisciplinary Nanoscience Center, Department of Chemistry; Quai Ernest-Ansermet 24, University of Geneva<br>Chierotti, Michele; Università di Torino, Chemistry<br>Matsuo, Motoaki ; Tohoku University, Institute for Materials Research<br>Li, Guanqiao; Tohoku University, Institute for Materials Research<br>Gobetto, Roberto; University of Torino, Chemistry I.F.M.<br>Jensen, Torben; University of Aarhus, Interdisciplinary Nanoscience Center, Department of Chemistry<br>Černý, Radovan; Quai Ernest-Ansermet 24, University of Geneva<br>Orimo, Shin-Ichi; Tohoku University, Institute for Materials Research<br>Baricco, Marcello; Universita di Torino, Department of Chemistry |
| | |

# $Li_5(BH_4)_3NH$, Lithium Rich Mixed Anion Complex Hydride

Anna Wolczyk[1,2],Biswajit Paik[3], Toyoto Sato[2], Carlo Nervi[1], Matteo Brighi[4], SeyedHosein Payandeh GharibDoust[4,5], Michele Chierotti[1], Motoaki Matsuo[2], Guanqiao Li[3], Roberto Gobetto[1], Torben R. Jensen[5], Radovan Černý[4], Shin-ichi Orimo[2,3] and Marcello Baricco[1,a)]

[1]*Department of Chemistry and NIS, University of Turin, Via P.Giuria 9, I-10125 Torino, Italy*
[2]*Institute for Materials Research, Tohoku University, Katahira 2-1-1, Sendai, 980-8577, Japan*
[3]*WPI-Advanced Institute for Materials Research (WPI-AIMR), Tohoku University, Katahira 2-1-1, Sendai, 980-8577, Japan*
[4]*Laboratoire de Cristallographie, DQMP, Université de Genève, quai Ernest-Ansermet 24, CH-1211, Geneva 4, Switzerland*
[5]*Interdisciplinary Nanoscience Center (iNANO) and Department of Chemistry, University of Åarhus, Langelandsgade 140, DK-8000 Åarhus C, Denmark.*

[a)]Electronic mail: marcello.baricco@unito.it

Abstract

In this paper, the $Li_5(BH_4)_3NH$ complex hydride, obtained by ball milling $LiBH_4$ and $Li_2NH$ in various molar ratio, has been investigated. Using X-ray powder diffraction analysis the crystalline phase has been indexed with an orthorhombic unit cell with lattice parameters $a$ = 10.2031(3), $b$ = 11.5005(2) and $c$ = 7.0474(2) Å at 77 °C. The crystal structure of $Li_5(BH_4)_3NH$ has been solved in space group *Pnma*, and refined coupling DFT and synchrotron radiation X-ray powder diffraction (SR-XPD) data of a $3LiBH_4$:$2Li_2NH$ ball milled sample after annealing. Solid state NMR measurements confirmed the chemical shifts calculated by DFT from the solved structure. The DFT calculations confirmed the ionic character of this Lithium rich compound. Each $Li^+$ cation is coordinated by three $BH_4^-$ and one $NH^{2-}$ anion in a tetrahedral configuration. The room temperature ionic conductivity of the new orthorhombic compound is close to$10^{-6}$ S/cm at room temperature, with activation energy of 0.73 eV.

Keywords: Energy storage, $LiBH_4$-$Li_2NH$ system, complex hydride, X-ray powder diffraction, Li-ion conductivity, activation energy.

## 1. Introduction

Lithium-based complex hydrides have been suggested as a promising class of materials for future energy storage applications.[1] While some of them have attractive $H_2$ storage capacity (e.g. $LiBH_4$[2] and $LiNH_2$[3]), some turned out to be Li-ion super-ionic conductors (e.g. $LiBH_4$[4] and $Li_2NH$[5]) with a prospect of being used as electrolyte in the all-solid-state Li-ion battery. To improve further the properties, the concept of anion mixing was introduced.[6,7]

The structure of potential solid-state electrolytes typically contains polyanions $[AB_y]^{n-}$ with covalent A-B bonds (e.g. $PO_4^{3-}$ and $SO_4^{2-}$),[8] where the cation conductivity is promoted by rotation of $[AB_y]^{n-}$ units. As a consequence, corresponding activation energies are decreased by the commonly named "paddle-wheel" mechanism.[9] This approach, originally designed for lithium or sodium salts containing dynamically disordered complex anions, was extended to higher boranes, such as $[B_{10}H_{10}]^{2-}$ or $[B_{12}H_{12}]^{2-}$ in Na-based compounds.[10] In fact, superionic conductivity, firstly evidenced in metal borohydrides based on the complex anion $[BH_4]^-$, was recently observed also in these compounds.[11]

Mixed anion complex hydrides may provide a means to tune the hydrogen sorption, as well as the ionic conductivity.[12] As an example, the combination of $LiNH_2$:$LiBH_4$[7,13,14,15] may be promising for hydrogen storage[16] and can be used as a fast Li-ion conductors in the solid state (in 1:1 - $Li_2BH_4NH_2$ and 3:1 - $Li_4BH_4(NH_2)_3$ mole ratio).[17,7] The formation of a new compound has been recently reported for the $1LiBH_4$:$1Li_2NH$ composition by D. R. Hewett.[18] This is an example where single and double charged anions are combined in a Li-based complex hydride, which has been seldom considered in the literature.[10] Motivated by this result, we experimentally examined the $LiBH_4$:$Li_2NH$ system to determine the structure of this new complex hydride and to explore its ion conduction properties.

In this work, various samples in $LiBH_4$-$Li_2NH$ system were synthesized by ball milling and a detailed examination of the structure and properties was performed through a combination of X-ray powder diffraction, solid state nuclear magnetic resonance and ac impedance spectroscopy coupled with density functional theory calculations. In the whole explored composition range, a mixed anion orthorhombic phase has been identified. From suitable annealing treatment of ball-milled $3LiBH_4$:$2Li_2NH$ mixtures, a nearly single phase sample has been obtained, allowing the determination of the crystal structure corresponding to a $Li_5(BH_4)_3NH$ stoichiometry. Li-ion conductivity turned out intermediate between those of parent compounds.

## 2. Experimental

Samples were prepared by ball milling (Fritsch Pulverisette7, milling duration 5 h, 400 rpm, Ar environment) $LiBH_4$ (purity ≥90.0%, purchased from Aldrich) and $Li_2NH$ in 1:2, 1:1, 3:2, 2:1 and 3:1 molar ratios. The parent $Li_2NH$ was prepared by decomposing commercially available $LiNH_2$ (purity ≥ 95.0%, purchased from Aldrich) isothermally at 550 ºC for 48 h under dynamic vacuum.[19]

The structural characterization of the $LiBH_4$:$Li_2NH$ mixtures was carried out by X-ray powder diffraction (XPD) (PANalytical X'PERT with Cu Kα radiation). Variable temperature synchrotron radiation X-ray powder diffraction (SR-XPD) data has been collected at Swiss-Norwegian Beamlines of the European Synchrotron Radiation Facility in Grenoble, France. A Dectris Pilatus M2 detector[20] was used for data acquisition at a wavelength of 0.7143 Å calibrated using the external NIST SRM660b $LaB_6$ standard. The data were collected between RT and 127 ºC. The temperature was controlled with a hot air blower and the 2-dimensional images were integrated and treated with the local program Bubble. Indexing of diffraction patterns was performed with TREOR97[21] and PIRUM[22] software. Crystal structure solutions were obtained by global optimization in direct space using the software Fox[23] and refined with the Rietveld method using TOPAS.[24]

Periodic lattice calculations based on density-functional theory (DFT) were performed by means of Quantum Espresso version 5.1.2,[25] adopting the Generalized Gradient Approximation (GGA) functional PW86PBE,[26] with the inclusion of the exchange-hole dipole moment (XDM) dispersion correction method[27] for modeling weak interactions. XDM dispersion energies were calculated adopting the damping parameters optimized for similar inorganic systems.[15] Calculations were performed adopting the Kresse-Joubert Projected Augmented Wave pseudopotentials.[28] Cut-offs of 60 Ry and 80 Ry were used for structural optimizations and GIPAW[29] NMR calculations, respectively. The Brillouin zones were automatically sampled with the Monkhorst–Pack scheme,[30] in a similar approach as previously described.[31] Geometry optimization and NMR chemical shift calculations were performed with a grid mesh of 1×1×2. The theoretical absolute magnetic shielding (σ) values were converted into chemical shifts (δ) relative to the absolute magnetic shielding of the reference substance ($LiBH_4$ for $^7Li$, $^1H$ and $^{11}B$, $LiNH_2$ for $^{15}N$) computed at the same level, following a similar procedure reported elsewhere.[15] Gaussian 09 Rev. D.01[32] was employed for gas phase calculations at B3LYP/def2-TZVP level, including the D3 version of Grimme's dispersion method with the Becke-Johnson damping scheme.[33] The natures of stationary points were confirmed by normal-mode analysis.

Solid-state NMR measurements were run on a Bruker Advance II 400 instrument operating at 400.23, 155.54, 128.41 and 40.56 MHz for $^1H$, $^7Li$, $^{11}B$ and $^{15}N$, respectively. $^1H$ magic-angle spinning (MAS) spectra were acquired in a 2.5 mm probe with a spinning speed of 32 kHz using the DEPTH sequence for suppressing the probe background signal [90° pulse = 1.8 μs; optimized recycle delay = 1.5s; 64 transients]. $^7Li$, $^{11}B$ and $^{15}N$ spectra were recorded at room temperature at the spinning speed of 12 kHz with cylindrical 4 mm o.d. zirconia rotors with sample volume of 80 μL. For $^7Li$ and $^{11}B$ MAS spectra, single-pulse excitation (SPE) or DEPTH (for suppressing the probe background signal) sequences were used [90° pulse = 3.75 ($^{11}B$) and 2.35 μs ($^7Li$); recycle delays = 0.2 s (both $^7Li$ and $^{11}B$); 128 transients]. $^{15}N$ CPMAS spectra were acquired with a ramp cross-polarization pulse sequence (contact time = 3ms; a 1H 90° pulse = 3.05 μs, recycle delays = 1.5s, 71100 transients) with two-pulse phase modulation (TPPM) decoupling scheme (rf field = 75 kHz). The $^1H$, $^7Li$, $^{11}B$ and $^{15}N$ chemical shift scales were calibrated using adamantane ($^1H$ signal at 1.87 ppm), 1 M aqueous LiCl ($^7Li$ signal at 0.0 ppm), $NaBH_4$ ($^{11}B$ signal at −42.0 ppm with respect to $BF_3{\cdot}Et_2O$) and $(NH_4)_2SO_4$ ($^{15}N$ signal at δ = −355.8 ppm with respect to $CH_3NO_2$) as external standards, respectively.

The Li-ion conductivity was measured by electrochemical impedance spectroscopy (EIS) in a HP4192A LF impedance analyzer (frequency range 5 Hz ÷ 2 MHz, applied voltage 50 mV) and a Novocontrol sample cell BDS 1200, at every 10 K temperature interval over a temperature window from room temperature up to 373 K. The pellet (diameter 6.35 mm, thickness 0.7 mm) was obtained by pressing the ball milled powder in a axial hydraulic press at 800 MPa (density > 94 % of the calculated value) and measured in a symmetrical cell Au/(sample)/Au. Impedance data were analyzed by EqC software[34] following the deconvolution process and data validation described in ref. 35 on the third heating/cooling cycle to guarantee the reproducibility of the measurements.

## 3. Results and Discussion

### 3.1 Synthesis and Phase Analysis

The XPD patterns obtained from the ball milled compositions $x$LiBH$_4$:$y$Li$_2$NH with the molar ratios ($x$:$y$) selected as 1:2, 1:1, 3:2 and 2:1 are shown in Figure 1. PXD analysis shows that ball milling causes a reaction between LiBH$_4$ and Li$_2$NH, in all samples, which results in the formation of a new phase. Corresponding diffraction peaks are more clearly visible for 1LiBH$_4$:1Li$_2$NH (1:1) and 3LiBH$_4$:2Li$_2$NH (3:2) compositions. On the other hand, for 2:1 sample, the reaction seems to be incomplete, because of the presence of both reagents and of the mixed compound. Nevertheless, on the basis of the relative intensities of XPD peaks, an increasing relative amount of the mixed compound with respect to Li$_2$NH, can be evidenced by increasing the $x$:$y$ ratio, reaching a maximum for the 3:2 sample.

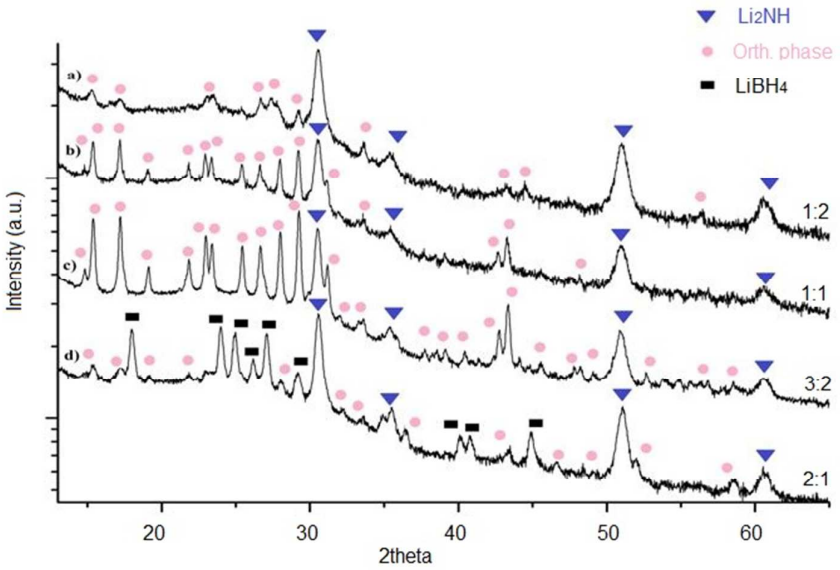


Figure 1. XPD patterns obtained from ball milled xLiBH$_4$:yLi$_2$NH mixtures with molar combination ratio (x:y) selected as a) 1:2,b) 1:1, c) 3:2 and d) 2:1 after 5 h ball milling. Intensity is in logarithmic scale.

The diffraction pattern of the novel compound was indexed in an orthorhombic unit cell, as previously reported for the 1LiBH$_4$:1Li$_2$NH composition by D. R. Hewett.[18] The systematic absences indicated the space group *Pnma* or its non-centrosymetrical subgroup $Pn2_1a$. As the orthorhombic phase could not be isolated nor formed pure and the stoichiometry was unknown, authors in ref. 18 did not propose any structural model.

For this reason, a ball milled 3LiBH$_4$:2Li$_2$NH sample was annealed at 117 °C for 2 hours to promote the formation of the orthorhombic mixed anion phase and it was further studied at Swiss-Norwegian Beamlines of ESRF by variable temperature SR–XPD. Results of measurements are shown in Figure 2, during heating up to 131 °C and then cooling down to room temperature. At room temperature, the orthorhombic phase coexists together with small amount of unreacted reactants. An unidentified peak is also present around 12.7 °, which disappears after annealing up to ~90 °C. The orthorhombic compound clearly melts at 117 °C and recrystallizes back on cooling. After cooling at room temperature, a single phase pattern for the mixed anion compound has been obtained, together with the unidentified peak, which forms again.

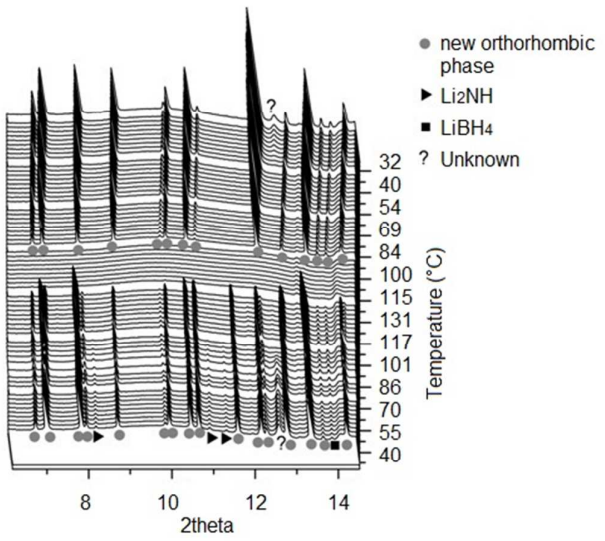


Figure 2. *In situ* SR-PXD data for $3LiBH_4$:$2Li_2NH$ sample first heated up to 131 °C at 5 °C $min^{-1}$ and then cooled down to room temperature.

### 3.2 Crystal structure analysis

The powder pattern measured at 77 °C on heating was used for crystal structure solution, combining Rietveld refinement and DFT optimization. The structure was modeled with two semi-rigid ideal tetrahedra $BH_4$ with one common refined B - H distance of 1.13 Å, and with one linear NH group with the N-H distance fixed to 1.03 Å. The position and orientation of the rigid units were allowed to vary in agreement with the space group symmetry as well as the positions of three lithium atoms. The convergence was improved by using appropriate anti-bump interatomic distances. The two impurities ($LiBH_4$ and $Li_2NH$) were modeled with their known structural models and a peak of an unidentified phase have been excluded from the refinement. From the analysis of diffraction data and DFT calculations, the existence of a $[Li_5NH]^{3+}$ unit in the solid phase was suggested. Experimental data, together with corresponding Rietveld refinement, are reported in Figure SI1. The lattice parameters of the orthorhombic phase turned out as a = 10.2031(3), b = 11.5005(2) and c = 7.0474(2) Å at 77 °C. Similar lattice parameters were previously reported for the $1LiBH_4$:$1Li_2NH$ composition by D. R. Hewett,[18] where Pawley fit allowed to obtained lattice parameters $a$ = 10.146(9), $b$ = 11.483(1) and $c$ = 7.030(4) Å. The amount of $LiBH_4$, $Li_2NH$ and orthorhombic phase turned out to be 2, 5 and 93 wt %, respectively.

Rietveld refinement of diffraction data and DFT calculations led to a structure model with the composition of $Li_5(BH_4)_3NH$. The occurrence of this compound in huge amount in a sample with $3LiBH_4$:$2Li_2NH$ stoichiometry suggests the need of an excess of $Li_2NH$ to promote the synthesis of $Li_5(BH_4)_3NH$ compound by ball milling. In fact, after ball milling of a $2LiBH_4$:$1Li_2NH$ mixture, a significant amount of parent $LiBH_4$ and $Li_2NH$ is still present in the sample (Figure 1). An attempt to obtain the pure compound by ball milling a $3LiBH_4$:$1Li_2NH$ mixture resulted in unreacted $LiBH_4$ together with a tiny amount of $Li_5(BH_4)_3NH$ (Figure SI2). In addition, the existence of a composition range of stability for $Li_5(BH_4)_3NH$ cannot be excluded.

The obtained structural model was further optimized by solid state DFT calculations using the fixed lattice with unit cell parameters from Rietveld refinement, and with atomic positions fully relaxed. The optimization confirmed the *Pnma* space group, and the optimized model was very close to that one obtained by Rietveld refinement, and differing in slightly rotated $BH_4$ units. Optimization with fully relaxed lattice cell confirmed the agreement between experimental and computational data (DFT optimized cell volume was only 1.5% smaller than the experimental one). The determined composition and unit cell volume per formula unit for $Li_5(BH_4)NH$ are reasonably agreed with consideration of ionic filling fraction for complex hydrides.[36] The crystal structure of $Li_5(BH_4)_3NH$ is shown in the Figure 3 and reported in SI. It contains the imide anion coordinated by a square pyramidal cluster of five Li atoms as a particular structural feature. It forms unusual $Li_5NH$ structure with Li atoms at the vertex of a square pyramid, the N atom in the center of

the square base and the H bonded to N pointing out perpendicularly to the base. As the compound is Lithium rich (five cations per four complex anions), the coordination of both borohydride anions is also five-fold, but more irregular than the coordination of imide. All three Li atoms are in strongly deformed tetrahedral coordination containing three $BH_4^-$ and one $NH^{2-}$ anion.

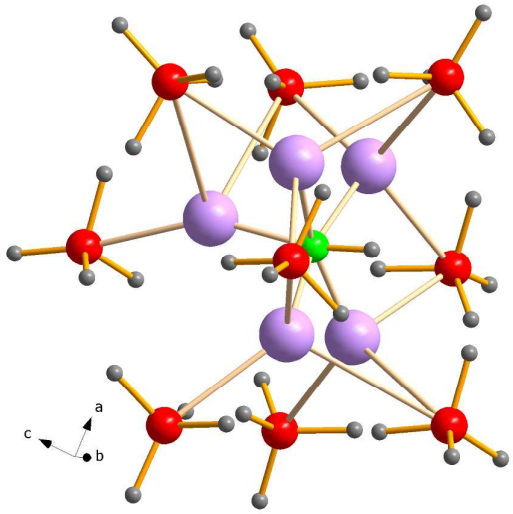


Figure 3. Crystal structure of $Li_5(BH_4)_3NH$ showing the square pyramidal $[Li_5(NH)]^{3+}$ complex cation counter balanced by three $BH_4^-$ complex anions as basic structural units. In colours: red – B atom, grey – H atom, purple – Li atom, green – N atom.

The unusual ionic $Li_5NH$ core pushed us to explore its properties at the molecular level in the gas phase, using the program Gaussian. Calculations in the gas phase confirmed the arrangement of the $[Li_5(NH)]^{3+}$ core. When surrounded by four $BH_4$ units, the anion $[Li_5(BH_4)_4(NH)]^-$, with an overall $C_{2v}$ symmetry, has been found after geometry optimization. The HOMO and HOMO-1 orbitals of $[Li_5(BH_4)_4(NH)]^-$ are essentially the $p_x$ and $p_y$ N atomic orbitals (Figure 4) and have the same energy. This particular arrangement suggests that the surrounding $[BH_4]^-$ moieties play a crucial role in the solid state by stabilizing the $[Li_5(NH)]^{3+}$ core, which is of pure ionic nature with the exception of the covalent N-H bond (see SI).

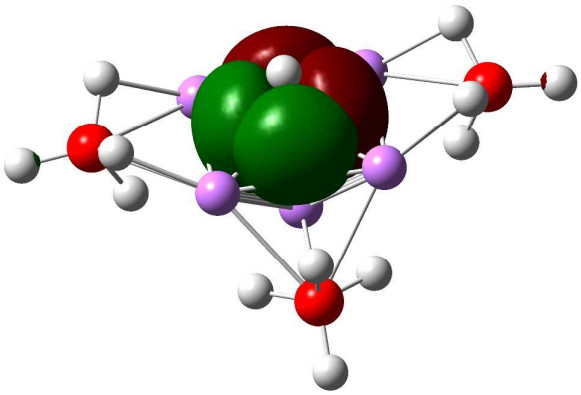

Figure 4. HOMO and HOMO-1 of the DFT optimized geometry of $[Li_5(BH_4)_4(NH)]^-$. One $[BH_4]^-$ unit is hindered behind the orbitals. In colours: red – B atom, grey – H atom, purple – Li atom. Green and claret volumes are the visualization of, respectively, positive and negative values of HOMO and HOMO-1 orbitals.

The square pyramidal $[Li_5(NH)]^{3+}$ core polymerizes into the crystal structure of $Li_5(BH_4)_3NH$, and keeps its character of complex cation counter balanced by three $BH_4^-$ complex anions. The only other known example of a complex cation was found in $Al_3Li_4(BH_4)_{13}$ as a tetrahedral $[Li_4(BH_4)]^{3+}$.[37]

$Li_5(BH_4)_3NH$ is the first reported mixed anion salt containing borohydride and imide anions. It can be compared with $Li_4(BH_4)(NH_2)_4$[17] with imide replaced by amide anion. Both compounds are of ionic character, but while the former is

based on packing of a big complex cation $[Li_5(NH)]^{3+}$ and small complex anion $BH_4^-$, the latter is based on packing of small cation $Li^+$ and complex anions $BH_4^-$ and $NH_2^-$ resulting in close to *ccp* of anions. The formation of complex cation $[Li_5(NH)]^{3+}$ corresponds to higher coordinating power of imide compared to amide.

### 3.3 NMR

A further characterization of the $Li_5(BH_4)_3NH$ compound has been performed by $^1H$, $^7Li$ and $^{11}B$ MAS and $^{15}N$ CPMAS SSNMR measurements and the results are shown in Figure 5. At the same time, corresponding chemical shifts have been calculated for the DFT optimized periodic structure. The corresponding experimental and calculated chemical shifts are listed in Table 1. The four molecules in the cell unit resulted into 8 set of non-magnetically equivalent hydrogens having a relative abundance of 4:8:4:8:8:8.8:4, as shown in Table 1. The last four hydrogens (calculated and experimental chemical shifts at -2.7 and -3.4 ppm, respectively) are assigned to the NH unit. The $^1H$ MAS spectrum (Figure 5a) is characterized by a main resonance at -0.1 ppm attributed to the 12 hydrogen atoms of the $BH_4^-$ and a small peak at -3.4 ppm due to the NH. Integral values obtained from deconvolution analysis confirm the assignment. Excellent agreement is observed between experimental and calculated $^1H$ data (Table 1). $^7Li$ MAS spectrum (Figure 5b) shows a single large resonance (LWHM=350 Hz) at 1.6 ppm in agreement with the computed chemical shifts, which give an averaged value of 1.35 ppm (Table 1). The spinning sideband pattern is very small, indicating a relatively low quadrupolar contribution attributed to a substantial high symmetry of the lithium environments. As expected, the $^{11}B$ MAS spectrum (Figure 5c), characterized by a single signal at -39.5 ppm, is similar to that of pure $LiBH_4$ (-41.8 ppm).[15] The large manifold of spinning sideband can be related to the asymmetric distribution of the $Li^+$ cations around the $BH_4^-$ units assuming a perfect tetrahedral structure of the $BH_4^-$ anion. The natural abundance $^{15}N$ CPMAS spectrum (Figure 5d) is characterized by a single resonance at 58.4 ppm, in agreement with the presence of two very similar independent NH sites in the unit cell. The similarity of the independent sites is confirmed also by the similarity of the computed chemical shifts, 51.6 and 52.1 ppm (Table 1). GIPAW calculations of chemical shifts outline a good agreement between the experimental and the weighted average value of computed chemical shift, confirming the accuracy of the determined structure for the $Li_5(BH_4)_3NH$ compound.

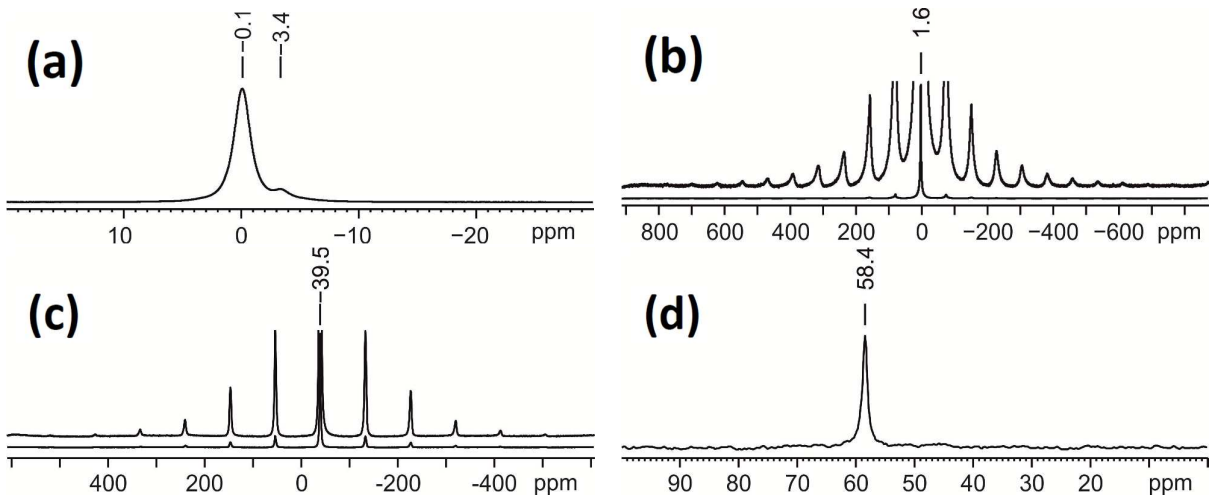


Figure 5. SSNMR spectra for a $3LiBH_4$:$2Li_2NH$ ball-milled sample annealed at 117 °C for 2 hours. (a) $^1H$ (400.23 MHz) MAS spectra acquired at 32 kHz. (b) $^7Li$ (155.54 MHz) MAS spectra acquired at 12 kHz (c) $^{11}B$ (128.41 MHz) MAS spectra acquired at 12 kHz. (d) $^{15}N$ (40.56 MHz) MAS spectra acquired at 9 kHz.

Table 1. SSNMR chemical shifts. $<\delta_{iso}>$: experimental values for $3LiBH_4:2Li_2NH$ ball-milled sample annealed at 117 °C for 2 hours. $\delta_{iso}$: weighted mean of the computed non-equivalent calculated for the orthorhombic $Li_5(BH_4)_3NH$ phase. # = number of equivalent nuclei in the cell.

| | $^1$H | | | $^7$Li | | | $^{11}$B | | | $^{15}$N | | |
|---|---|---|---|---|---|---|---|---|---|---|---|---|
| **Compound** | $<\delta_{iso}>$ | # | $\delta_{iso}$ | $<\delta_{iso}>$ | # | $\delta_{iso}$ | $<\delta_{iso}>$ | # | $\delta_{iso}$ | $<\delta_{iso}>$ | # | $\delta_{iso}$ |
| **Exp** | -0.1<br>-3.4 | | | 1.6 | | | -39.5 | | | 58.4 | | |
| $Li_5(BH_4)_3NH$ | -0.1 | 4 | 0.1 | 1.35 | 4 | -0.03 | -41.6 | 4 | -39.4 | 51.8 | 2 | 52.1 |
| | | 8 | -0.5 | | 8 | 1.93 | | 8 | -42.64 | | 2 | 51.6 |
| | | 4 | 0.0 | | 8 | 1.45 | | | | | | |
| | | 8 | 0.7 | | | | | | | | | |
| | | 8 | -0.1 | | | | | | | | | |
| | | 8 | -0.3 | | | | | | | | | |
| | | 8 | -0.6 | | | | | | | | | |
| | -2.7 | 4 | -2.7 | | | | | | | | | |

### 3.4 Lithium Ion Conductivity

Figure 6 shows the ionic conductivity of $3LiBH_4:2Li_2NH$ sample (annealed after ball milling) measured in a symmetrical cell Au/(sample)/Au within a temperature range 27 - 100 ºC. An equivalent circuit composed by a four series element was used. The first consist in a resistor (R) in parallel with a constant phase element (CPE). The more resistive element was associated to the orthorhombic $Li_5(BH_4)_3NH$ phase, whereas the remaining two elements were interpreted as contribution from the impurity of parent compounds. The fourth element is a CPE which model the polarization due to the imperfect contact between the pellet and the electrode. Even if the contributions from the impurities are always, at least, one order of magnitude less resistive than the main one, the total resistance was used to calculate the ionic conductivity of the whole pellet. For comparison, the ionic conductivity data measured for starting $LiBH_4$ and $Li_2NH$ have been also reported in Figure 6. From the temperature dependence of Li-ion conductivity, an activation energy of 0.73 eV has been estimated for $Li_5(BH_4)_3NH$ compound.

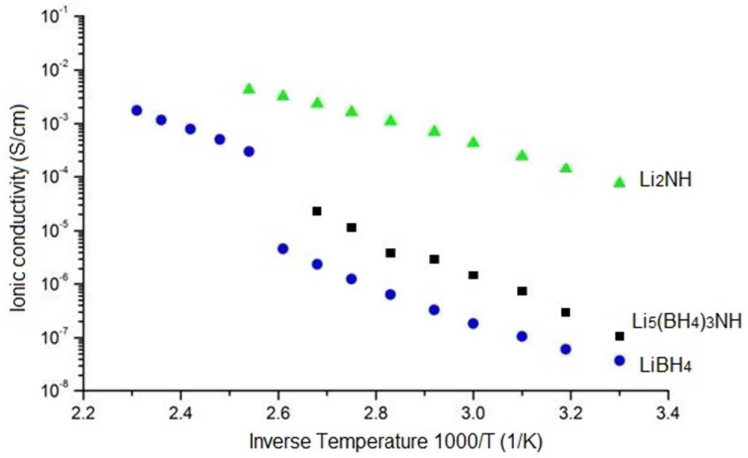


Figure 6. Ionic conductivity of the $3LiBH_4:2Li_2NH$ sample after 5 h ball milling and 2h annealing at 120 °C (squares– black in colour). Ionic conductivity of the precursors $Li_2NH$ (triangles – green in colour) and $LiBH_4$ (dots – blue in colour) have been added for comparison.

The room temperature conductivity of the $Li_5(BH_4)_3NH$ compound is less than one order of magnitude higher than that in $LiBH_4$, but it is about three orders of magnitude lower than $Li_2NH$. The observed differences and similarities in the Li-ion conductivity in the three complex hydrides, viz., $LiBH_4$, $Li_2NH$ and $Li_5(BH_4)_3NH$, may be explained by ionic conduction mechanisms. A rotational motion of the translationally static $BH_4^-$ anions enhances the mobility of $Li^+$ ions in case of high temperature $LiBH_4$,[38] whereas Frenkel pair defects or charged vacancies are considered in case of $Li_2NH$.[39] For the orthorhombic $Li_5(BH_4)_3NH$, the Li-ion conductivity may be significantly affected by both anions.

It is worth noting that the ionic conductivity in the $Li_5(BH_4)_3NH$ phase, is comparable to that, of some recently reported binary complex hydrides including, for example, $LiBH_4$-LiX solid solutions X = Cl, Br, I)[40] and $Li_4(BH_4)(NH_2)_3$.[13] This may suggest that Li-based complex hydrides containing a combination of $BH_4^-$ and $NH^{2-}$ anions may be potential choices to promote high ionic conduction at room temperature.[40]

**4. Conclusions**

In this work, novel complex hydride have been prepared by ball milling $LiBH_4$ and $Li_2NH$ in various molar ratios. New orthorhombic compound - $Li_5(BH_4)_3NH$ - with lattice parameters $a$ = 10.2031(3), $b$ = 11.5005(2) and $c$ = 7.0474(2) Å at 77 °C, was observed by XRD in 1:2, 1:1, 3:2 and 3:1 molar ratios samples. Its crystal structure was solved in the space group *Pnma* from temperature dependent synchrotron radiation X-ray powder diffraction data. The cation coordination and interatomic distances point to the ionic character of the structure with the imide anion coordinated by a square pyramidal cluster of five Li atoms as a particular structural feature. The structure and bonding character has been confirmed by the periodic and molecular DFT calculations. Excellent agreement is observed between experimental and calculated $^1H$ data in solid state NMR spectra. The spinning sideband pattern of $^7Li$ is very small, indicating a relatively low quadrupolar contribution, attributed to a substantial high symmetry of the lithium environments. The large manifold of $^{11}B$ spinning sideband can be related to the asymmetric distribution of the $Li^+$ cations around the $BH_4^-$ units, assuming a perfect tetrahedral structure of the $BH_4^-$ anion. The natural abundance $^{15}N$ spectrum is characterized with the presence of two very similar independent NH sites in the unit cell.

DFT played a crucial role in analysis of the $Li_5NH$ core confirming the final structure of $Li_5(BH_4)_3NH$. The plane wave optimized structure is very close to the experimental data (only 1.5% smaller in volume), differing in slightly rotated $BH_4$ units. GIPAW calculations of chemical shifts outline a good agreement between the experimental and the weighted average value of computed chemical shift.

Electrochemical impedance spectra measured on $Li_5(BH_4)_3NH$ showed a Li-ion conductivity close to $10^{-6}$ S/cm at room temperature, with an activation energy of 0.73 eV. These results suggest the complex hydrides containing a combination of $BH_4^-$ and $NH^{2-}$ anions may be a potential choice to reach room temperature super-ionic conductivity, with better thermal stability compared to other complex hydrides containing multi-anions. Further studies may pave ways to design new binary and ternary complex hydrides with superior properties for energy storage applications.

**Acknowledgements**

European Marie Curie Actions under ECOSTORE grant agreement no. 607040 is acknowledged for supporting this work. The work has been funded by the Japan Society for the Promotion of Science (JSPS) KAKENHI Grant Numbers 25220911, 26820311 and 16K06766 and Grant-in-Aid for Research Fellow of JSPS No. 10604. RC acknowledges the support of the Swiss National Science Foundation. Technical assistances from Ms. N. Warifune is also greatly acknowledged. The authors acknowledge the Diamond Light Source, the Swiss-Norwegian Beamlines of ESRF and the Materials Science beamline of the SLS for the allocation of beamtime and excellent support with the data collection.

**References**

1. Orimo S.; Nakamori Y.; Eliseo J. R.; Züttel A.; Jensen C. M. Complex Hydrides for Hydrogen Storage. *Chem. Rev*. **2007,** 107, 4111–4132.

2. Orimo S.; Nakamori Y.; Kitahara G.; Miwa K.; Ohba N.; Towata S.; Zuttel A. Dehydriding and rehydriding reactions of $LiBH_4$. *J. Alloys Compd*, **2005,** 404-406, 427-430.

3. Chen P.; Xiong Z. T; Luo J. Z.; Lin J. Y.; Tan K. L. Interaction of hydrogen with metal nitrides and imides. *Nature* **2002,** 420, 302-304.

4. Matsuo M.; Nakamori Y.; Orimo S.; Maekawa H.; Takamura H. Lithium superionic conduction in lithium borohydride accompanied by structural transition. *Appl. Phys. Lett*. **2007**, 91, 224103-224106.

5. Boukamp B. A.; Huggins R. A. Ionic conductivity in lithium imide. *Phys. Letts*. **1979**, 72, 464-466.

6. Anderson P. A.; Chater P. A.; Hewett D. R.; Slater P. R. Hydrogen storage and ionic mobility in amide–halide systems, *Faraday Discuss*. **2011**, 151, 271-284.

7. Matsuo M.; Remhof A.; Martelli P.; Caputo R.; Ernst M.; Miura Y.; Sato T.; Oguchi H.; Maekawa H.; Takamura H. et al. Complex hydrides with $(BH_4)^-$ and $(NH_2)^-$ anions as new lithium fast-ion conductors. *J. Amer. Chem. Soc*. **2009**, 131, 16389–16391.

8. Yabuuchi N.; Kubota K.; Dahbi M. Komaba S. Research development on sodium-ion batteries. *Chem. Rev*. **2014**, 114, 11636–11682.

9. Jansen M. Volume Effect or Paddle Wheel Mechanism-Fast Alkali Metal Ionic Conduction in Solids with Rotationally Disordered Complex Anions. *Angew. Chem. Int. Ed*. **1991**, 30, 1547–1558.

10. Sadikin Y.; Brighi M.; Schouwink P.; Černý R. Superionic Conduction of Sodium and Lithium in Anion-Mixed Hydroborates $Na_3BH_4B_{12}H_{12}$ and $(Li_{0.7}Na_{0.3})_3BH_4B_{12}H_{12}$ *Adv. Energy Mater.* **2015**, 5, 1501016.

11. a) Martelli P.; Remhof A.; Borgschulte A.; Ackermann R.; Strassle T.; Embs J. P.; Ernst M.; Matsuo M.; Orimo S.; Züttel A. Rotational motion in $LiBH_4$/LiI solid solutions. *J. Phys. Chem. A*. **2011**, 115, 5329-5334.

b) Verdal N.; Udovic T. J.; Rush J. J.; Wu H.; Skripov A. V. Evolution of the reorientational motions of the tetrahydroborate anions in hexagonal $LiBH_4$–LiI solid solution by high-Q quasielastic neutron scattering. *J. Phys. Chem. C.* **2013**, 117, 12010–12018.

c) Skripov A. V.; Soloninin A. V.; Ley M. B.; Jensen T. R.; Filinchuk Y. Nuclear magnetic resonance studies of $BH_4$ reorientations and Li diffusion in $LiLa(BH_4)_3Cl$. *J. Phys. Chem. C.* **2013**, 117, 14965–14972.

12. Borgschulte A.; Jones M. O.; Callini E.; Probst B.; Kato S.; Züttel A., David W. I. F.; Orimo S. Surface and bulk reactions in borohydrides and amides. *Energy Environ. Sci*. **2012**, 5, 6823-6832.

13. Aoki M.; Miwa K.; Noritake T.; Kitahara G.; Nakamori Y.; Orimo S.; Towata S. Destabilization of $LiBH_4$ by mixing with $LiNH_2$. *Applied Physics A* **2005**, 80, 1409-1412.

14. Chater P. A.; Anderson P. A.; Prendergast J. W.; Walton A.; Mann V. S. J.; Book D.; David W. I. F.; Johnson S.R.; Edwards P. P. Synthesis and characterization of amide–borohydrides: New complex light hydrides for potential hydrogen storage. *J. Alloys Compd*. **2007**, 446–447, 350–354.

15. Wolczyk A.; Pinatel E. R.; Chierotti M. R.; Nervi C.; Gobetto R.; Baricco M. Solid-state NMR and thermodynamic investigations on $LiBH_4$-$LiNH_2$ system. *Int. J. Hydrogen Energy*, **2016**, 41, 14475-14483.

16. Meisner G. P.; Scullin M. L.; Balogh M. P.; Pinkerton, F. E.; Meyer M. S. Hydrogen release from mixtures of lithium borohydride and lithium amide: a phase diagram study. *J. Phys. Chem. B* **2006**, 110, 4186-4192.

17. Filinchuk Y. E.; Yvon K.; Meisner G. P.; Pinkerton F. E.; Balogh M. P. On the composition and crystal structure of the new quaternary hydride phase $Li_4BN_3H_{10}$. *Inorg. Chem*. **2006**, 45, 1433-1435.

18. Hewett D. R. Mixed Anion Amides for Hydrogen Storage, PhD thesis, University of Birmingham, U.K., **2012**.

19. Noritake T.; Nozaki H.; Aoki M.; Towata S.; Kitahara G.; Nakamori Y.; Orimo S. Crystal structure and charge density analysis of $Li_2NH$ by synchrotron X-ray diffraction. *J. Alloys Compd*. **2005**, 393, 264–268.

20. Dyadkin V.; Pattison P.; Dmitriev V.; Chernyshov. D. A new multipurpose diffractometer PILATUS@SNBL. *J. Synchrotron Radiat.* **2016**, 23, 3, 825–829.

21. Werner P. E.; Eriksson L.; Westdahl M. TREOR, a semi-exhaustive trial-and-error powder indexing program for all symmetries. *J. Appl. Cryst*. **1985**, 18, 367-370.

22. Werner P. E. A fortran program for least–squares refinement of crystal–structure cell dimensions. *Ark. Kemi.* **1969**, 31, 513-516.

23. Favre-Nicolin V.; Černý R. FOX, `free objects for crystallography': a modular approach to ab initio structure determination from powder diffraction. *J Appl. Cryst.* **2002**, 35, 734-743.

24. Coelho A. A. TOPAS-academic, http://www.topas-academic.net.

25. Giannozzi P.; Baroni S.; Bonini N.; Calandra M.; Car R.; Cavazzoni C.; et al. QUANTUM ESPRESSO: a modular and open-source software project for quantum simulations of materials. *J Phys Condens Matter* **2009**, 21, 395502-395521.

26. a) Perdew J.; Burke K.; Ernzerhof M. Generalized gradient approximation made simple. *Phys. Rev. Lett.* **1996**, 77, 3865-3868; b) Perdew J. P.; Wang Y. Density-functional approximation for the correlation energy of the inhomogeneous electron gas. *Phys. Rev. B* **1986**, 33, 8800-8822.

27. a) Otero-de-la Roza A.; Johnson E. R. Non-covalent interactions and thermochemistry using XDM-corrected hybrid and range-separated hybrid density functionals. *J. Chem. Phys.* **2013**, 138, 204109; b) Otero-de-la Roza A.; Johnson E. R.; DiLabio G. A. Halogen bonding from dispersion-corrected density-functional theory: The role of delocalization error. *J. Chem. Theory Comput.* **2014**, 10, 5436-5447.

28. Kresse G.; Joubert D. From ultrasoft pseudopotentials to the projector augmented-wave method. *Phys. Rev. B* **1999**, 59, 1758-1775.

29. Pickard C. J.; Mauri F. All-electron magnetic response with pseudopotentials: NMR chemical shifts. *Phys. Rev. B* **2001**, 63, 245101.

30. Monkhorst H. J.; Pack J.D. Special points for Brillouin-zone integrations. *Phys. Rev. B* **1976**, 13, 5188-5192.

31. Franco F.; Baricco M.; Chierotti M. R.; Gobetto R.; Nervi C. Coupling Solid-State NMR with GIPAW ab Initio Calculations in Metal Hydrides and Borohydrides. *J. Phys. Chem. C* **2013**, 117, 9991-9998.

32. Frisch M. J.; Trucks G. W.; Schlegel H. B.; Scuseria G. E.; Robb M. A.; Cheeseman J. R.; Scalmani G.; Barone V.; Mennucci B.; Petersson G. A.; et al. Gaussian 09, revision D.01, Gaussian, Inc., Wallingford, CT, **2009**.

33. Grimme S.; Ehrlich S.; Goerigk L. Effect of the damping function in dispersion corrected density functional theory. *J. Comp. Chem.* **2011**, 32, 1456-1465.

34. Boukamp B. A. A package for impedance/admittance data analysis. *Solid State Ionics* **1986**, 18, 136-140.

35. Boukamp B. A. Electrochemical impedance spectroscopy in solid state ionics: recent advances. *Solid State Ionics* **2004**, 169, 65-73.

36. T. Sato T.; Takagi S.; Deledda S.; Hauback B. C.; Orimo S. Extending the applicability of the Goldschmidt tolerance factor to arbitrary ionic compounds. *Sci. Rep.* **2016**, 6, 23592.

37. Lindemann I.; Ferrer R. D.; Dunsch, L.; Filinchuk Y.; Cerny R.; Hagemann H.; D'Anna V.; Lawson Daku M. L.; Schultz L; Gutfleisch O. Al3Li4 (BH4) 13: A Complex Double□Cation Borohydride with a New Structure. *Chemistry A Eur. J.* **2010**, 16, 8707 – 8712.

38. Matsuo M.; Orimo S. Lithium Fast□Ionic Conduction in Complex Hydrides: Review and Prospects. *Advanced Energy Materials* **2011**, 1, 161–172.

39. Li W.; Wu G.; Xiong Z.; Feng Y. P.; Chen P. $Li^+$ ionic conductivities and diffusion mechanisms in Li-based imides and lithium amide. *Phys Chem*. **2012**, 14, 1596-1606.

40. Maekawa H.; Matsuo M.; Takamura H.; Ando M.; Noda Y.; Karahashi T.; Orimo S. Halide-stabilized $LiBH_4$, a room-temperature lithium fast-ion conductor. *J. Amer.Chem. Soc*. **2009**, 131, 894-895.